ELSEVIER

Journal of Chromatography A, 926 (2001) 187–198

JOURNAL OF CHROMATOGRAPHY A

www.elsevier.com/locate/chroma

High-performance liquid chromatography–electrospray ionization mass spectrometry and multiple mass spectrometry studies of hyperforin degradation products

N. Fuzzati, B. Gabetta, I. Strepponi*, F. Villa

Indena SpA, Laboratori Ricerca e Sviluppo, Via Don Minzoni 6, 20090 Settala (Milan), Italy

Abstract

The alcoholic extract of the aerial parts of *Hypericum perforatum* L. finds wide application because of its antidepressant activity. The extract contains a number of constituents with documented biological activity including chlorogenic acid, a broad range of flavonoids, naphthodianthrones and phloroglucinols. Hyperforin and adhyperforin are the major phloroglucinol constituents found in the lipophilic fraction of the extracts. Since the stability of hyperforin has been shown to be limited, an investigation of the hyperforin degradation products using HPLC–electrospray ionization mass spectrometry and multiple mass spectrometry was undertaken.

Keywords: *Hypericum perforatum*; Hyperforin; Adhyperforin; Furohyperforin; Phloroglucinols

1. Introduction

Hypericum perforatum L. is a medicinal plant already known as an anti-inflammatory and healing agent in traditional medicine. Nowadays, the alcoholic extract of its aerial parts finds wide application because of it antidepressant activity [1]. The extract contains a number of constituents with documented biological activity including chlorogenic acid, a broad range of flavonoids, naphthodianthrones and phloroglucinols [1,2]. Hyperforin and adhyperforin (Fig. 1) are the major phloroglucinol constituents found in the lipophilic fraction of the extract. Recent studies have suggested that hyperforin might be a critical component for the antidepressant activity of *H. perforatum* [3,4]. Several investigations have shown the presence of other minor hyperforin analogues in *H. perforatum* extracts [2,5,6]. Recently the structures of three oxidated derivatives of hyperforin have been reported (Fig. 1) [7–10]. Since pure hyperforin has been shown to be extremely sensitive to oxidation and, as it is generally unstable in solution [11,12], it is not clear whether the isolated compounds are natural products or artifacts of extraction/isolation procedures. A recent study has identified furohyperforin, also named orthoforin (Fig. 1), as the main oxidation product of hyperforin [10]. Furthermore, attempts to convert hyperforin into derivatives by treatment with oxygen or various oxidants gave overly complex mixtures [9].

High-performance liquid chromatography–mass spectrometry (HPLC–MS) has been shown to be a powerful tool for the studies of natural products and complex mixtures [13]. With this technique important structural information can be obtained on the metabolites on-line prior to isolation. In the present

*Corresponding author.

E-mail address: ivan.strepponi@indena.it (I. Strepponi).

0021-9673/01/$ – see front matter
PII: S0021-9673(01)01000-7

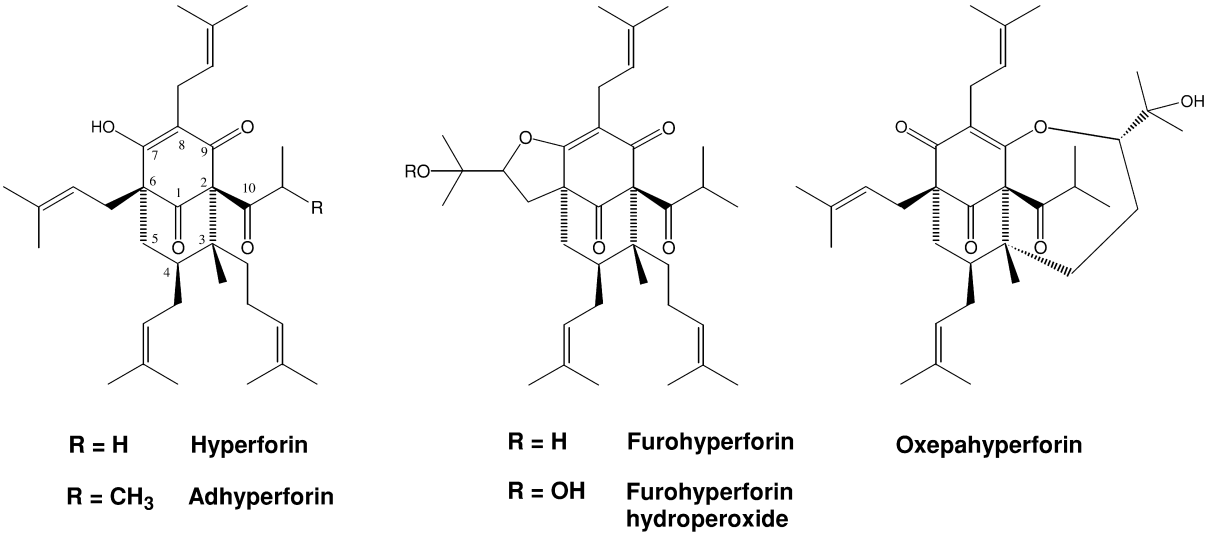

Fig. 1. Structures of hyperforin, adhyperforin and oxidation products of hyperforin.

work an investigation of different degradation conditions of hyperforin is described. The identification of several hyperforin degradation products was performed using HPLC–electrospray ionization mass spectrometry (ESI-MS) and multiple mass spectrometry (MS^n).

2. Experimental

2.1. Standards and samples

Hyperforin was isolated and characterized at the Indena Chemical Labs. Furohyperforin and furohyperforin peroxide were kindly furnished by Dr. L. Verotta, Istituto di Chimica Organica e Industriale, Universita' di Milano, Milan, Italy.

2.2. Solvents and reagents

Acetonitrile, methanol, ethanol, diethyl ether and *n*-hexane were HPLC grade from J.T. Baker (Deventer, The Netherlands); trifluoroacetic acid, Uvasol, from Merck (Darmstadt, Germany). Water was purified by a Milli-Q_{plus} system from Millipore (Milford, MA, USA).

2.3. Stability and degradation studies

About 100 mg of hyperforin was weighed in five different 50-ml volumetric flasks, dissolved and diluted to volume with methanol, ethanol, diethyl ether and *n*-hexane. The obtained solutions were stored at room temperature and under natural light exposure. About 100 mg of hyperforin was weighed in 50-ml volumetric flasks, dissolved and diluted to volume with methanol and kept at +4°C in the dark. After 2, 4, 20, 48 and 240 h, 1.0 ml of each solution was transferred into a 10-ml volumetric flask. The *n*-hexane and diethyl ether solutions were stripped with nitrogen and all the samples were diluted to volume with methanol and injected.

A round bottomed flask containing about 200 mg of hyperforin was kept open in an oil bath at 40°C for 1 week: samples of about 10.0 mg were accurately weighed into a 10-ml volumetric flask after 8, 24, 48 and 168 h, dissolved in methanol and injected.

2.3.1. HPLC–ESI-MS analyses

A Finnigan MAT (San Jose, CA, USA) LCQ ion trap mass spectrometer equipped with a Microsoft Windows NT data system and an ESI interface was used. The HPLC system included a Thermo Separation Product P4000 pump (San Jose, CA, USA) and a Thermo Separation Products UV6000LP diode

array detector. Separation was performed on a Zorbax Eclipse XDB-C_8 (5 μm) column (250×4.6 mm I.D.) from Agilent Technologies (Hewlett-Packard, Waldbronn, Germany). A step gradient of 0.01% (v/v) trifluoroacetic acid in water (A) and 0.01% (v/v) trifluoroacetic acid in acetonitrile (B) was used according to the following profile: 0–15 min, 20–15% A, 80–85% B; 15–25 min, isocratic 15% A, 85% B; 25–40 min, 15–0% A, 85–100% B; 40–50 min, isocratic 100% B. The flow-rate was 1.0 ml/min. The column temperature, controlled with a column heater–cooler HP Series 1100 from Hewlett-Packard, was set to 25°C. MS conditions were optimized in order to achieve maximum sensitivity. ESI conditions: source voltage 4.54 kV, sheath gas flow-rate 70, auxiliary gas flow 40 p.s.i., capillary voltage 25.2 V and capillary temperature 260°C (1 p.s.i.=6894.76 Pa). Full scan spectra from 150 to 2000 u in the positive ion mode were obtained (scan time 1 s). Ion trap conditions: acquisition in automatic gain control with a maximum-inject time of 200 ms. For the MS^n analyses a collision energy of 30 eV was used.

3. Results and discussion

HPLC–ESI-MS and MS^n analyses of hyperforin were undertaken in order to establish the fragmentation pathway. The MS spectrum (Fig. 2) of hyperforin displays an intense signal of the molecular ion $[M+H]^+$ at m/z 537. In the MS–MS (Fig. 2) spectrum, signals of several fragments, due to the successive losses of the alkylic chains such as

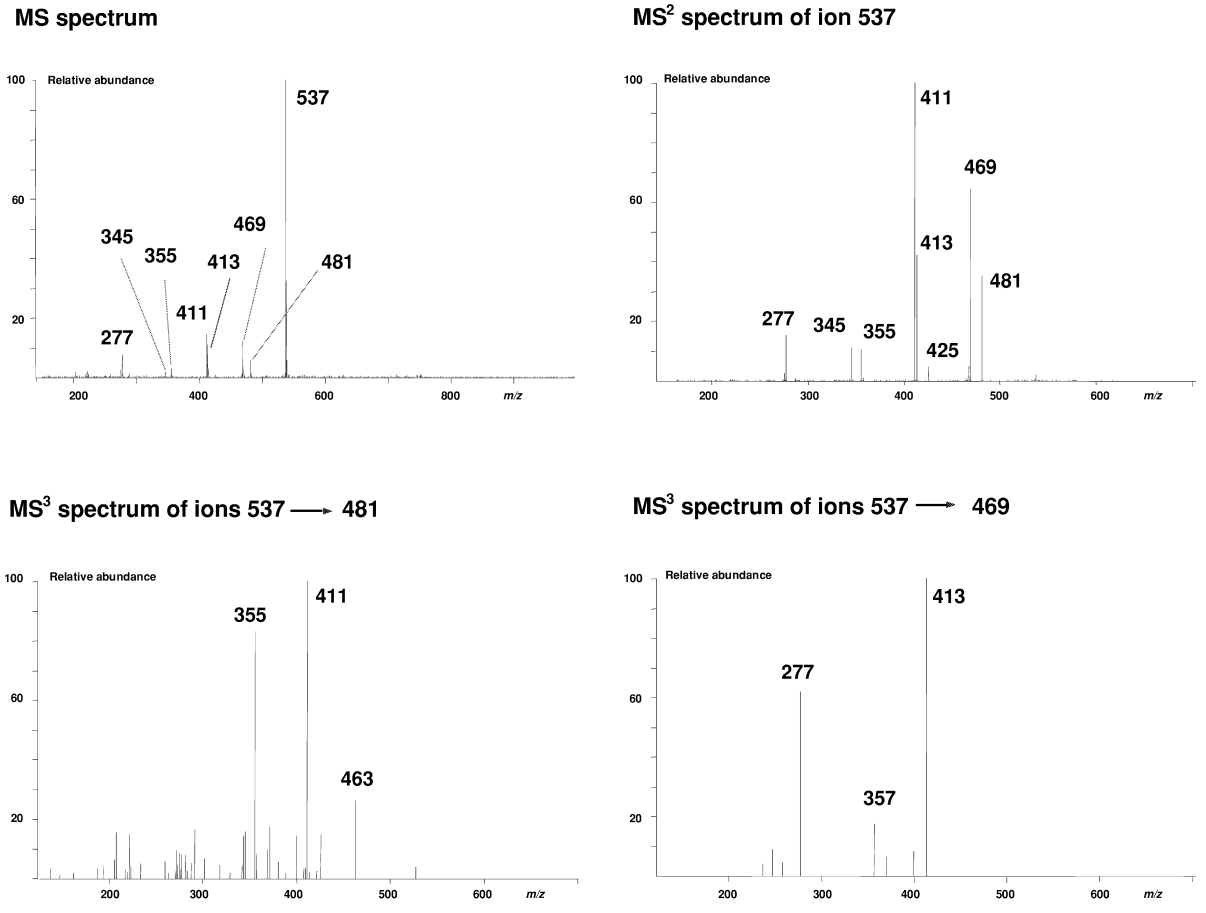

Fig. 2. HPLC–ESI-MS and MS^n spectra of hyperforin (peak 1) and proposed fragmentation pathway.

isoprene (−68 u), isobutene (−56 u), dimethylketene (−70 u) are detected. The study of the MS^3 spectra (Fig. 2) of ions at *m/z* 481 and 469 allows one to understand the fragmentation pathway of hyperforin (Fig. 3). The loss of isobutene is thought to involve a six-center concerted mechanism in which a transfer of the proton and keto–enol tautomerism takes place. The loss of the isoprene moiety is explainable with a concerted pericyclic mechanism and the concomitant opening of the hyperforin structure. A six-center concerted mechanism is believed to be involved also in the loss of the dimethylketene moiety. However, the change of hybridization of the carbon atom in position 2 from sp^3 to sp^2 is not compatible with the closed structure of hyperforin. For this reason a previous ring opening at the level of the bond in position C2–C3, achievable by a similar concerted mechanism, is proposed.

A concerted pericyclic mechanism is also involved in the formation of ions at *m/z* 345 and 355. Furthermore, the appearance of an ion at *m/z* 355 is accompanied by an intramolecular rearrangement.

The stability studies showed that hyperforin is stable at room temperature and at +4°C in methanol, ethanol and diethyl ether solution, while it suffers degradation at 40°C in the presence of air and in *n*-hexane solution.

The kinetics of degradation at 40°C in the presence of air (Fig. 4b) shows a 60% of degradation after 48 h. The chromatogram (Fig. 4a) exhibits the occurrence of two main degradation products: peaks 3 and 4. The HPLC–ESI-MS spectra of peaks 3 and 4 (Fig. 5) display intense signals of the molecular ions $[M+H]^+$ at *m/z* 569 and 553, corresponding to the previously isolated furohyperforin and furohyperforin hydroperoxide (Fig. 1) [8–10], respectively. The MS–MS analysis shows much simpler fragmentation of 3 and 4 (Fig. 5), in comparison to hyperforin. In fact, the initial losses of isobutene and isoprene and the loss of dimethylketene are not observed. The spectra show, instead, two consecutive losses of 204 and 56, respectively.

A hypothetical fragmentation pathway has been proposed for furohyperforin and its corresponding hydroperoxyde as well (Fig. 5). According to the proposed mechanism, the absence of the initial loss of isobutene is explained by the engagement of the oxygen atom in the formation of the tetrahydrofuran ring. The lack of the initial loss of the isoprene moiety as well, is explained by the blocking action of the tetrahydrofuran on the carbon atom in position C6. After the loss of 204 u, furohyperforin undertakes the loss of isobutene because the oxygen atom in position C9 can achieve an enolic form. The identification of 3 and 4 as furohyperforin and furohyperforin hydroperoxide, respectively, has been confirmed by injection of the standard compounds.

After 4 h in *n*-hexane solution the recovery of hyperforin was about 30% and after 20 h a full degradation was observed (Fig. 6b). The HPLC–ESI-MS chromatogram shows two main degradation products (peaks 7 and 8, Fig. 6a). The HPLC–ESI-MS spectra of peaks 7 and 8 (Fig. 7) display intense signals of the molecular ions $[M+H]^+$ at *m/z* 553 indicating that 7 and 8 are isomers of furohyperforin. However the MS and MS–MS spectra show a more complex fragmentation than that of furohyperforin. In particular the initial losses of isoprene and isobutene are observed. This behavior is justified by the presence of the tetrahydrofuran ring in position C7,C8 or C8,C9 (Fig. 7). Furthermore the MS and MS–MS spectra of peaks 7 and 8 exhibit the same fragment ions. The formation of the two isomers is explained by the keto–enol tautomerism of hyperforin, which permits the formation of the tetrahydrofuran ring in two different positions. Therefore, the hypothetical structures justify the more complex spectra compared to those of furohyperforin because the tetrahydrofuran ring in position C6,C8 or C8,C9 cannot exercise the same blocking action as the ring in position C6,C7. The proposed fragmentation pathway for the two isomers is shown in Figs. 8 and 9. In this case as well, concerted pericyclic mechanisms with intramolecular rearrangements are involved.

The HPLC–MS analysis of hyperforin starting material exhibits also a minor component (Peak 2). The MS spectrum of peak 2 displays an intense signal of the molecular ion $[M+H]^+$ at *m/z* 551. The MS–MS spectrum of peak 2 shows the same fragmentation pattern as hyperforin. Furthermore, the occurrence of fragments due to the ethylmethylketene loss (−84) allows the identification of peak 2 as adhyperforin. Under the investigated conditions, adhyperforin showed the same degradation behavior as hyperforin. In fact, after 48 h at

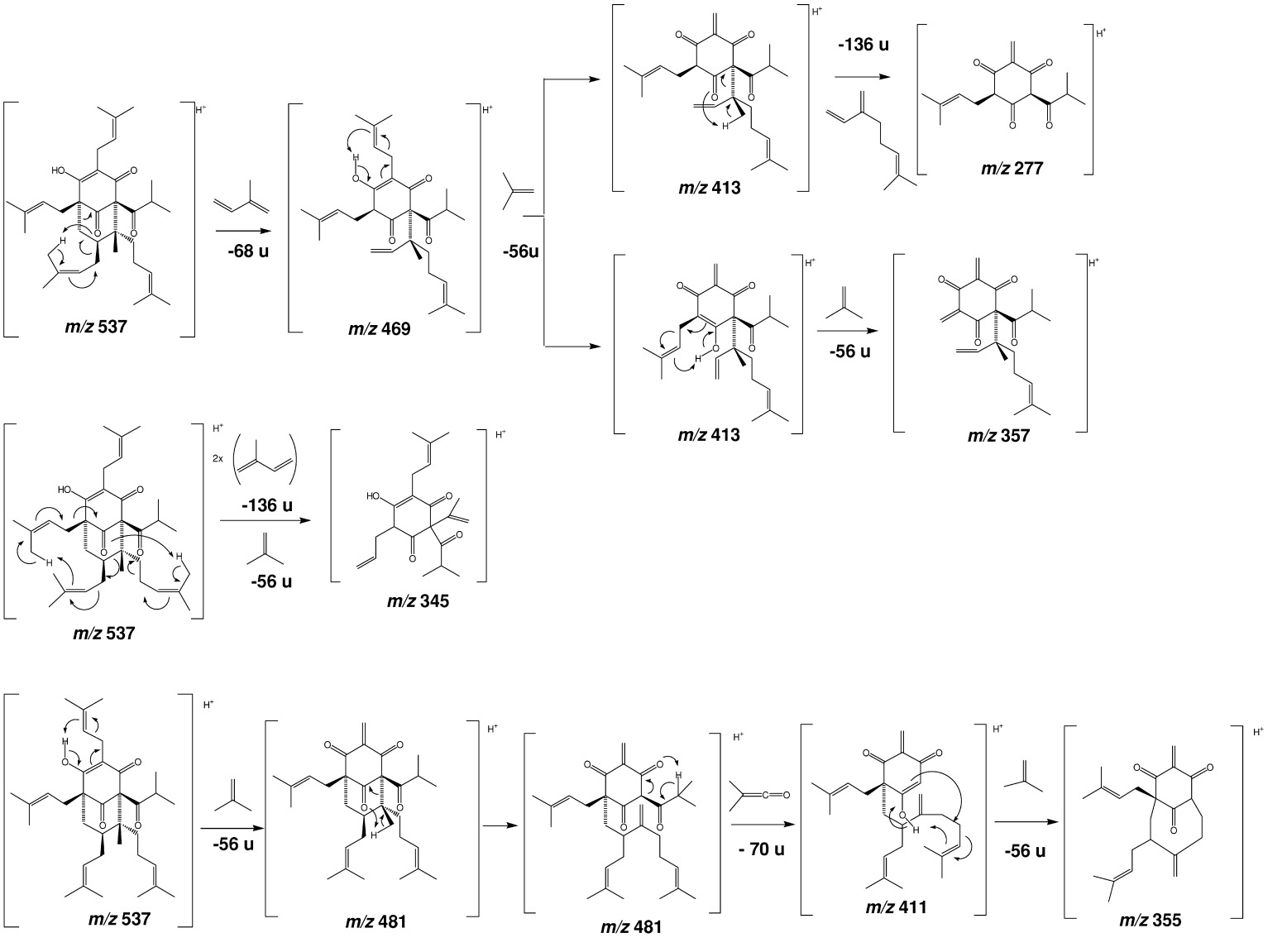

Fig. 3. Proposed fragmentation pathway of hyperforin (peak 1).

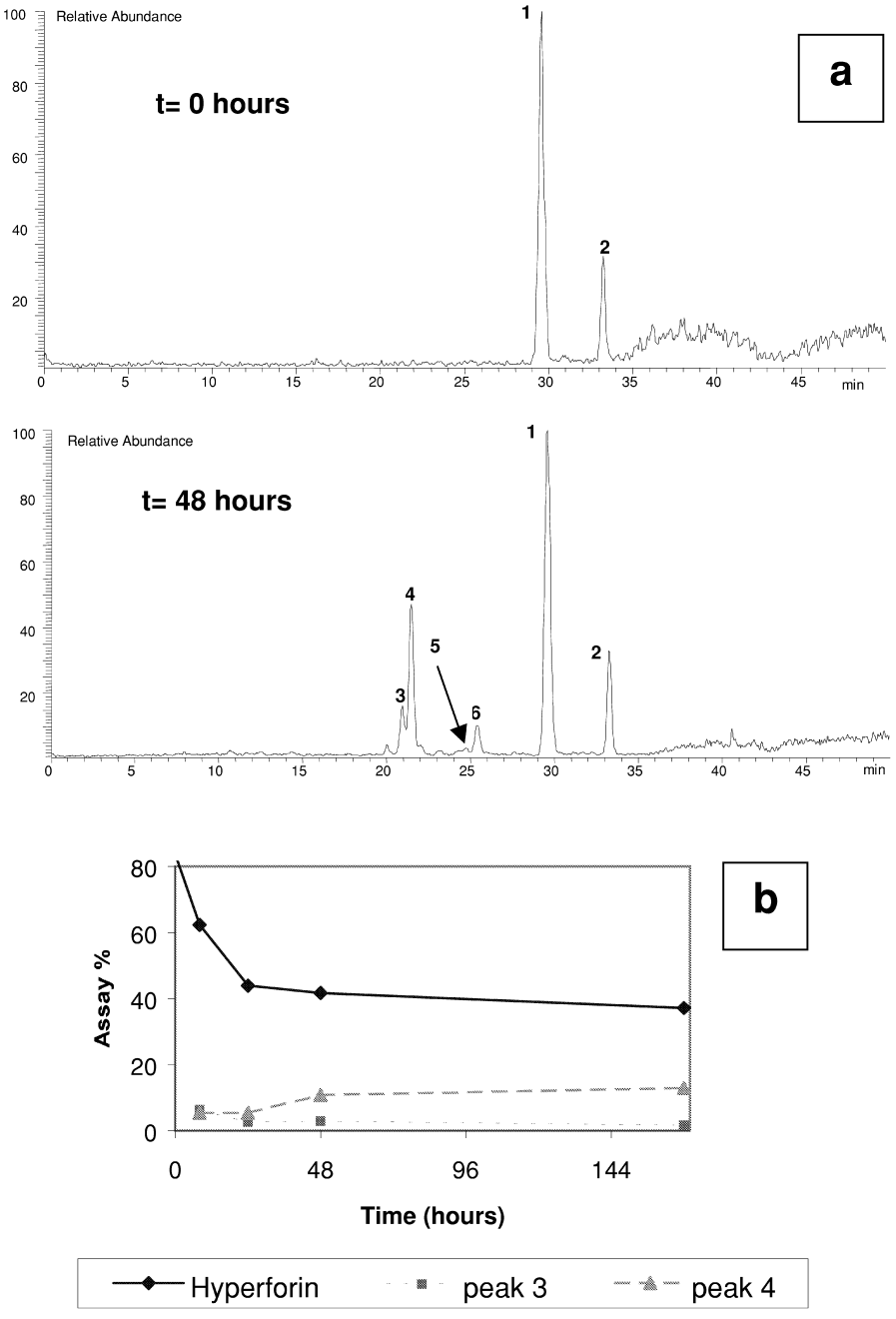

Fig. 4. (a) HPLC–ESI-MS profiles of hyperforin at $t=0$ and after 48 h at 40°C. (b) Kinetics of degradation of hyperforin at 40°C.

40°C in the presence of air, the HPLC–ESI-MS chromatogram showed, besides the previously described main degradation products of hyperforin, the occurrence of two minor components: peaks 5 and 6 (Fig. 4a). The HPLC–ESI-MS spectra of peaks 5 and 6 display intense signals at the level of the molecular ions $[M+H]^+$ at m/z 583 and 567, respectively. The MS–MS spectra of peaks 5 and 6, show the same

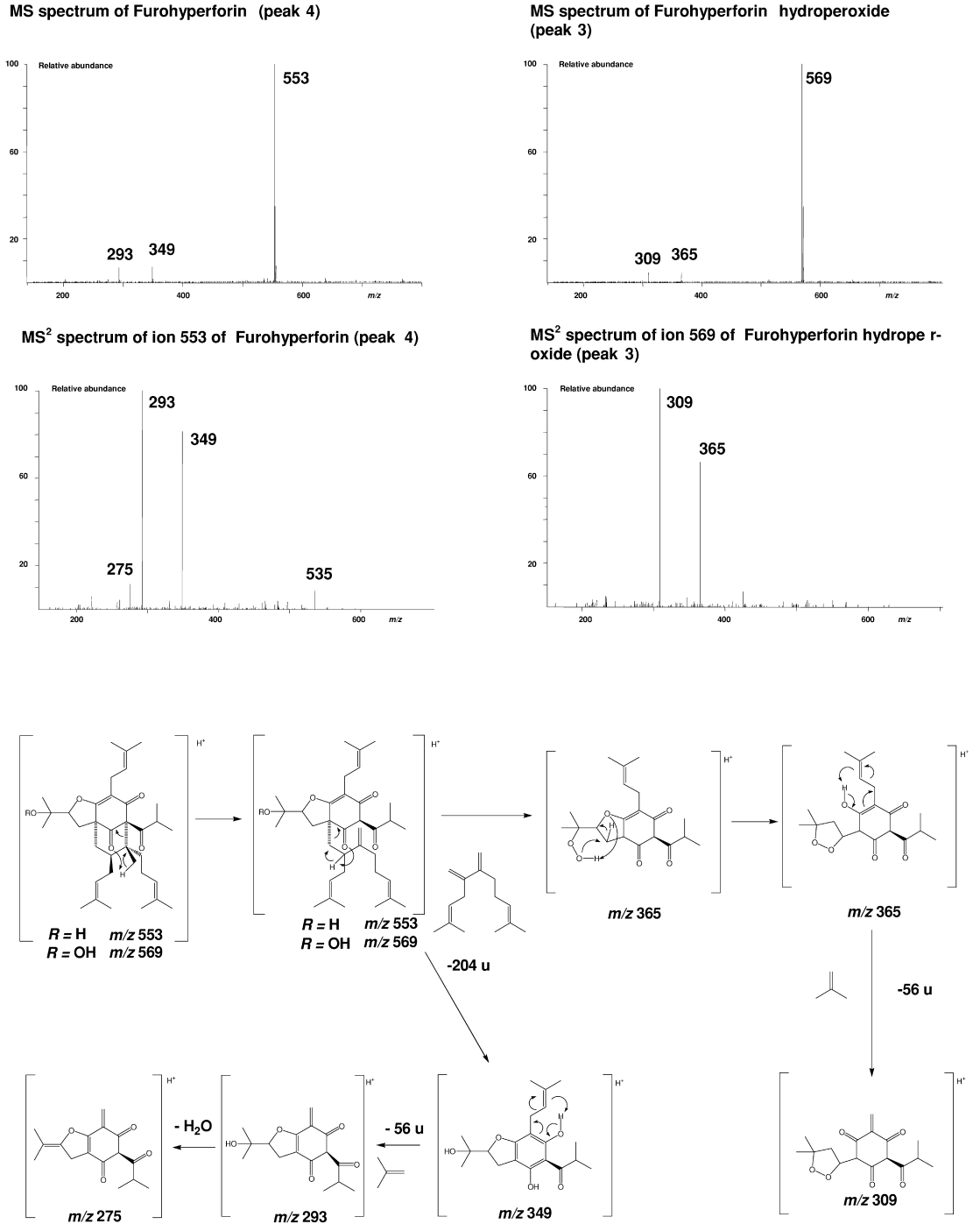

Fig. 5. HPLC–ESI-MS and MS–MS spectra of furohyperforin (peak 4) and furohyperforin hydroperoxide (peak 3) and proposed fragmentation pathway.

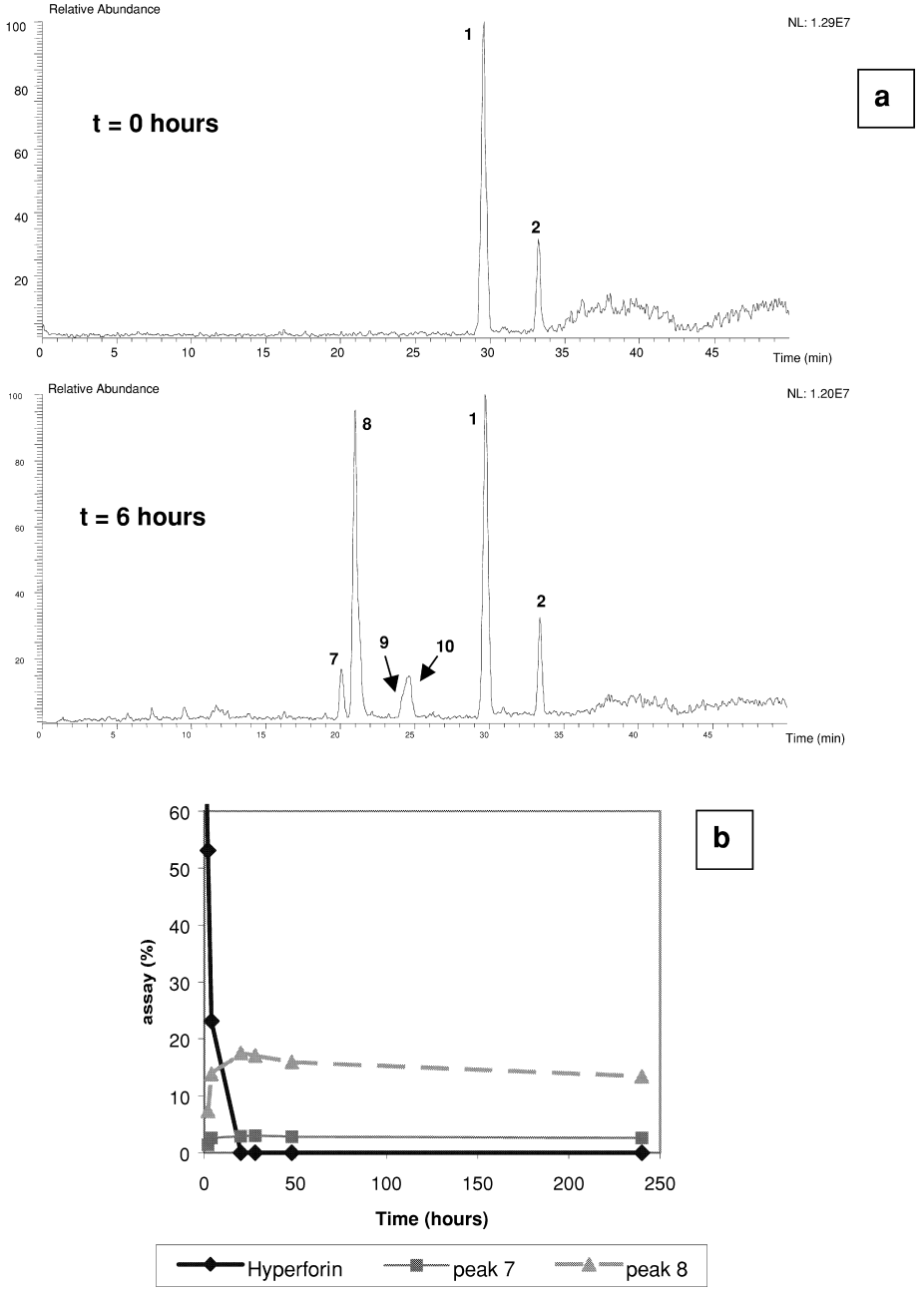

Fig. 6. (a) HPLC–ESI-MS profiles of hyperforin in *n*-hexane solution at $t=0$ and after 20 h. (b) Kinetics of degradation of hyperforin at 40°C in *n*-hexane solution.

losses of furohyperforin and furohyperforin hydroperoxide. This allows the identification of peaks 5 and 6 as furoadhyperforin and furoadhyperforin hydroperoxide, respectively.

Two other minor degradation products, peaks 9 and 10 (Fig. 6a) occur in the HPLC–ESI-MS chromatogram of the sample treated for 6 h in *n*-hexane solution. The HPLC–ESI-MS spectra of peaks 9 and

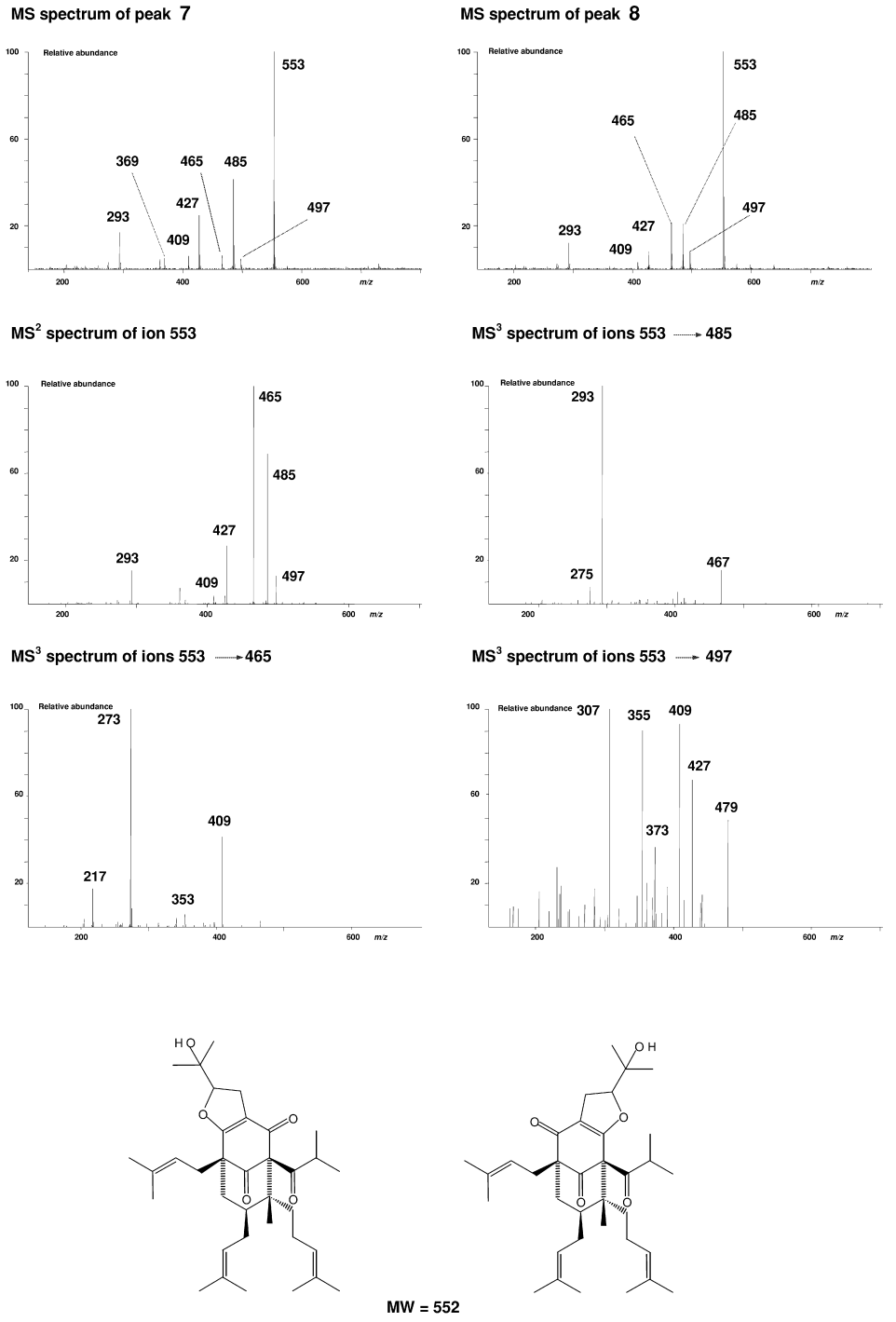

Fig. 7. HPLC–ESI-MS and MS^n spectra of peaks 7 and 8 and proposed structures. MW=Molecular mass.

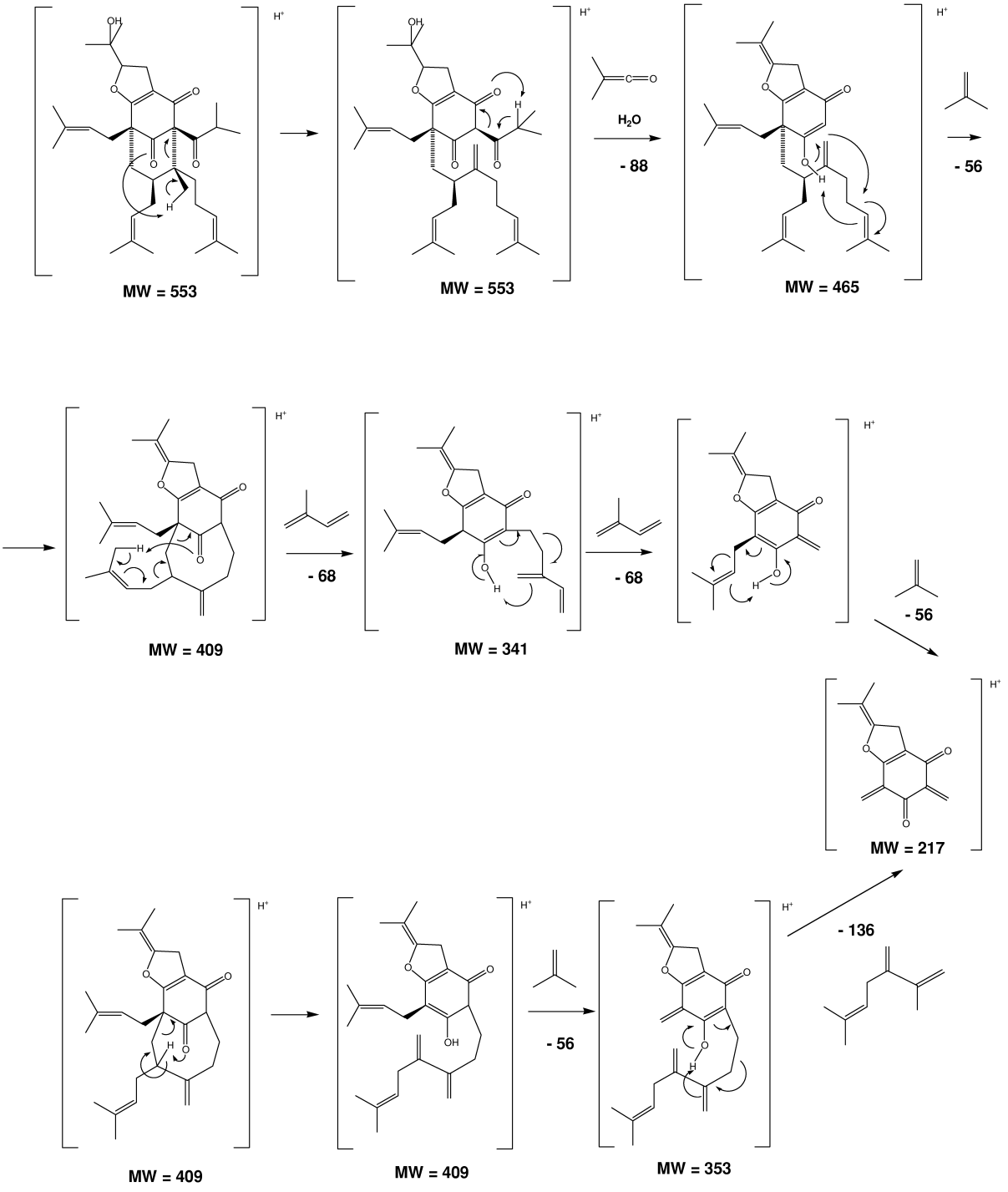

Fig. 8. Proposed fragmentation pathway of peaks 7 and 8.

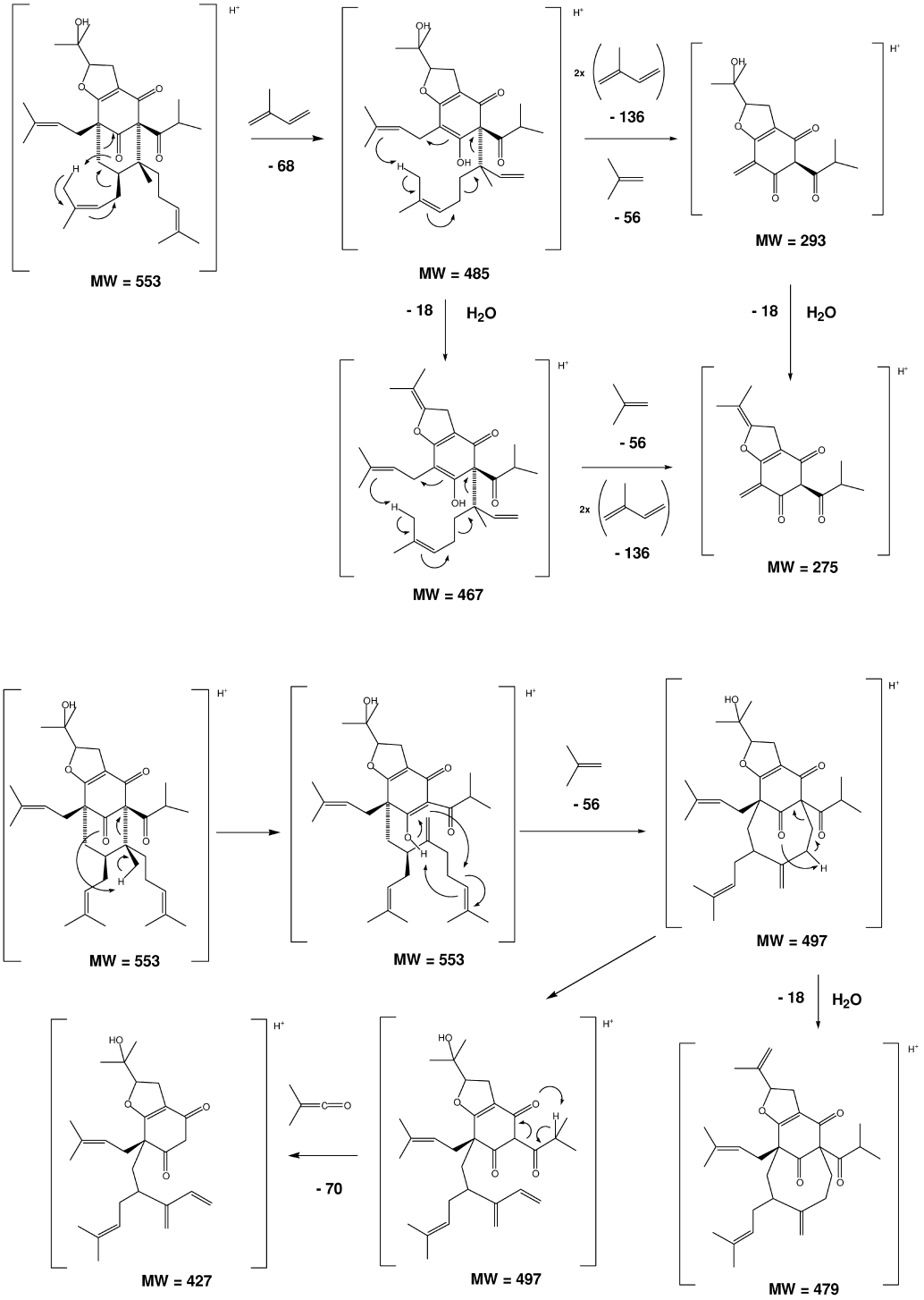

Fig. 9. Proposed fragmentation pathway of peaks 7 and 8.

Table 1
Identification of the degradation products of adhyperforin and hyperforin

Peak	Identification	RRT	$M+H^+$	M_r
1	Hyperforin	1	537	536
2	Adhyperforin	1.17	551	550
3	Furohyperforin hydroperoxide	0.70	569	568
4	Furohyperforin	0.75	553	552
5	Furoadhyperforin hydroperoxide	0.84	583	582
6	Furoadhyperforin	0.87	567	566
7	Furohyperforin isomer a	0.70	553	552
8	Furohyperforin isomer b	0.73	553	552
9	Furoadhyperforin isomer a	0.84	567	566
10	Furoadhyperforin isomer b	0.84	567	566

RRT=Relative retention time versus hyperforin.

10 display intense signals of the molecular ions $[M+H]^+$ at m/z 567. The MS^2 spectra of peaks 9 and 10, show the same fragmentation pattern of peaks 7 and 8 allowing to identify peaks 9 and 10 as furoadhyperforin isomers with the tetrahydrofuran ring in position C6,C8 or C8,C9.

Table 1 shows the identification of the degradation products of adhyperforin and hyperforin.

4. Conclusions

Hyperforin has been shown to be unstable at 40°C in the presence of air with the concomitant production of two main degradation products, that is furohyperforin and furohyperforin hydroperoxide. These two compounds, which were previously detected and isolated from *H. perforatum* extract, should be considered as artifacts. Hyperforin has been shown to be stable in protic solvents and unstable in apolar solvents such as *n*-hexane. In *n*-hexane two main degradation products are present which have been identified by HPLC–ESI-MS and MS^n as novel isomers of furohyperforin.

References

[1] E. Bombardelli, P. Morazzoni, Fitoterapia 66 (1995) 43.
[2] M. Brolis, B. Gabetta, N. Fuzzati, R. Pace, F. Panzeri, F. Peterlongo, J. Chromatogr. A 825 (1998) 9.
[3] C.A.J. Erdelmeier, Pharmacopsychiatry 31 (Suppl. 1) (1998) 2.
[4] S.S. Chatterjee, M. Noeldner, E. Koch, C.A.J. Erdelmeier, Pharmacopsychiatry 31 (Suppl. 1) (1998) 7.
[5] P. Maisenbacher, K.A. Kovar, Planta Med. 58 (1992) 351.
[6] M.D. Shan, L.H. Hu, Z.L. Chen, J. Nat. Prod. 64 (2001) 127.
[7] S. Trifunovic, V. Vajs, S. Macura, N. Juranic, Z. Djarmati, R. Jankov, S. Milosavljevic, Phytochemistry 49 (1998) 1305.
[8] L. Verotta, G. Appendino, E. Belloro, J. Jakupovic, E. Bombardelli, J. Nat. Prod. 62 (1999) 770.
[9] L. Verotta, G. Appendino, J. Jakupovic, E. Bombardelli, J. Nat. Prod. 63 (2000) 412.
[10] H.C.J. Orth, H. Hauer, C.A.J. Erdelmeier, P.C. Schmidt, Pharmazie 54 (1999) 1.
[11] H.C.J. Orth, C. Rentel, P.C. Schmidt, J. Pharm. Pharmacol. 51 (1998) 193.
[12] H.C.J. Orth, P.C. Schmidt, Pharm. Ind. 62 (2000) 60.
[13] J.L. Wolfender, K. Hostettmann, in: J.T. Arnason, R. Mata, J. Romeo (Eds.), Phytochemistry of Medicinal Plants, Plenum Press, New York, 1995, p. 189.